J.Cormier, F. Mauget
(Institut Pprime-ISAE ENSMA)
J-B Le Graverend*
(ONERA
Institut Pprime-ISAE ENSMA)
C. Moriconi
(Turbomeca-SAFRAN)
J. Mendez
(Institut Pprime-ISAE ENSMA)

E-mail: jonathan.cormier@ensma.fr

DOI: 10.12762/2015.AL09-07

Issues Related to the Constitutive Modeling of Ni-based Single Crystal Superalloys under Aeroengine Certification Conditions

This paper presents a constitutive modeling approach (the Polystar model) used to compute the viscoplastic behavior and the durability of high pressure turbine blades and vanes of aeroengines during complex thermomechanical histories typically encountered during certification procedures. This model is based on internal variables representing explicitly the microstructure evolutions occurring during very high temperature non-isothermal loading (e.g., dissolution/re-precipitation of the strengthening phase, dislocation recovery mechanisms, etc.) in a crystal viscoplasticity modeling framework. This article shows that the development of such a modeling tool requires a good characterization of fast microstructure evolutions, as well as in-service-type experiments (using burner rigs) able to reproduce the complex thermomechanical loading spectra. The capabilities of the model are illustrated, as well as its potential industrial applications and further developments are commented.

Introduction

Having robust life-prediction methods for the design of aeroengine high temperature components, such as turbine blades and vanes, are today highly desired by engine makers, especially when considering certification procedures. Indeed, the thermomechanical paths encountered by these components during certification are far more complex and severe than during their service life. As an example, the procedures for the certification of turboshaft engines for helicopters consist in mixing different engine regimes and repeated short very high temperature overheatings [1-4]. During these temperature peaks, high pressure turbine blades made of Ni-based single crystal superalloys are exposed to extreme conditions (temperatures close to their melting point). However, since these overheatings are short in duration (typically, from 5 to 150 seconds), the microstructure of the material is left out of equilibrium, leading to a transient mechanical response of the alloy [1, 2, 5-7]. As shown earlier by Cailletaud [8-10], a classical constitutive model in which the temperature dependence is only taken into account by the material parameters identified using isothermal experiments is not able to reproduce out of equilibrium states. Figure 1 illustrates this in the case of the polycrystalline Ni-based alloy IN 100, loaded under stress control non-isothermal LCF conditions [9]. It is especially observed in this figure that the modeling of the hysteresis loop using a classical viscoplastic approach* (dotted line in figure 1) over predicts the hysteresis width compared to the experimental loop (black dots). In order to obtain a better modeling of the behavior and life of the material, the proposed solution is to introduce additional internal variables accounting for microstructure evolutions, such as dissolution/precipitation of strengthening precipitates and their coarsening. This was already done by Cailletaud et al., as illustrated in figure 1, where such a "microstructure-sensitive" model was capable of accurately predicting the hysteresis loop after an overheating (continuous line in figure 1), even if the additional internal variables used by Cailletaud et al. were only tailored to capture the effect of microstructure evolutions at the macroscopic scale, without any actual representation of it (such as, e.g., precipitate size evolutions, volume fraction, or interparticle distances) [8-10].

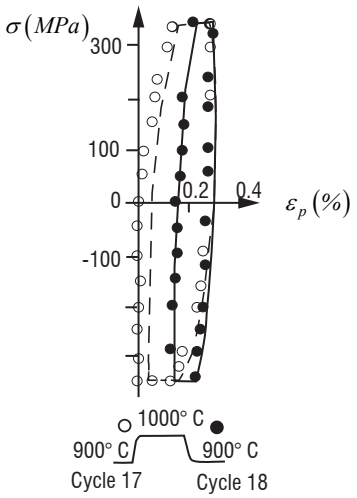

Figure 1 - Measured (circles) and calculated (lines) loops of the IN100 superalloy before and after an overheating at 1000°C lasting 120 s during the course of a fatigue test performed at 900°C, with $\Delta\sigma = 685MPa$ and $R = -1$ [9]. A decrease in the loop width is observed just after the overheating (black circles). The calculated loop without additional variables (dotted line) is not predictive of the post overheating loop compared to the model with additional variables (continuous line).

* Now at Texas A&M University, Department of Aerospace Engineering

Such a modeling approach has been re-used more recently at Institut Pprime, in collaboration with the Centre des Matériaux and ONERA, using a crystal plasticity framework and introducing internal variables accounting more accurately for microstructure evolutions [11-15]. The Polystar model was developed in 2007 to compute the creep elongation and life of Ni-based single crystal superalloys subjected to thermomechanical histories representative of those encountered in the most severely damaged sections of high pressure turbine blades during certification procedures (Accelerated Simulated Mission Endurance Testing - ASMET, or 150 hours engine tests). This model has been identified for different alloys and is currently under evaluation at SAFRAN-Turbomeca for 3D finite element calculations.

The aim of this article is to show that the development of such microstructure-sensitive models is necessarily accompanied by the performance of complex non-isothermal experiments and microstructure characterizations. Hence, after presenting the basic ingredients of the model and the microstructure evolutions occurring during very high temperature jumps, specific microstructure characterizations and burner testing experiments developed at Institut Pprime will be presented. The new burner rig facility developed (the MAATRE burner) to reproduce aeroengine operating conditions with a good control of both the applied temperature and the mechanical loading coupled with a monitoring of sample deformations will be briefly detailed [4, 16]. Then, the model performances under complex thermomechanical histories will be outlined, as well as some illustrative potential uses of the Polystar model in an industrial context. Finally, some on-going activities to improve the modeling approach will be discussed.

Basic ingredients of the model and the microstructural evolutions considered

Basic single crystal model and hardening modifications

The model used for the simulation of the non-isothermal creep behavior through additions of physically motivated internal variables is a crystal plasticity model that has been applied to numerous structural calculations of components, such as tubular testing samples [17] or single crystalline turbine blades made of superalloys [18]. The basic equations of this model under a small strain assumption are recalled below. γ^s is the viscoplastic shear on a given slip system s, v is its accumulated value (the derivative of the second being the absolute value of the first), τ^s is the resolved shear stress on slip system s, v is the accumulated viscoplastic strain and $\underline{\underline{\varepsilon}}^p$ is the viscoplastic strain tensor. The slip rate is determined (eq.(1)) by means of τ^s, the isotropic hardening r^s and the kinematic hardening x^s. $\underline{\underline{m}}^s$ is the orientation tensor calculated according to eq. (3), knowing the normal to the slip system plane $\underline{n}^s$ and the slip direction in this plane $\underline{l}^s$. Knowing the applied stress tensor $\underline{\underline{\sigma}}$, the resolved shear stress is calculated according to eq. (4) and then the viscoplastic strain tensor is determined using eq. (5). The damage evolution has been considered to occur at the slip system level. The damage scalar d_c^d is therefore introduced in eq. (1) using a concept of effective resolved shear stress. The damage evolution equation will be presented in § " Damage law " of this paper.

$$\dot{\gamma}^s = \left(\frac{\left| \tau^s - x^s \right| - r^s}{K\left(1 - d_c^s\right)} \right)^n sign\left(\tau^s - x^s\right) \quad (1)$$

$$\dot{v} = \left(\frac{2}{3} \left(\dot{\underline{\underline{\varepsilon}}}_p : \dot{\underline{\underline{\varepsilon}}}_p \right) \right)^{1/2} \quad (2)$$

$$\underline{\underline{m}}^s = \frac{1}{2}\left(\underline{n}^s \otimes \underline{l}^s + \underline{l}^s \otimes \underline{n}^s \right) \quad (3)$$

$$\tau^s = \underline{\underline{\sigma}} : \underline{\underline{m}}^s \quad (4)$$

$$\dot{\underline{\underline{\varepsilon}}}^p = \sum_s \dot{\gamma}^s \, \underline{\underline{m}}^s \quad (5)$$

As a second assumption, only octahedral slip systems (i.e. <110>{111} slip systems) will be considered (cubic slip - <110>{001} - and stacking fault systems - <112>{111} - systems are ignored).

To introduce the microstructure evolutions occurring during temperature changes [1, 5, 19-21], a new form of the isotropic hardening r^s is proposed in eq. (6). r^s depends on the isotropic state variable ρ^s on the slip system s (eq. (7)) and on τ_0^s, the critical resolved shear stress as usually defined. A non-linear saturating form of ρ^s is chosen in eq. 7 to account for the transition from the primary to the secondary creep stage. It represents the increase of the dislocation density in the γ channels and at the γ / γ' interfaces during the early stage of viscoplastic deformation and the critical dislocation density that can enter into γ channels [22, 23]. In addition, two new improvements have been made in the formulation of r^s:

- An Orowan $\tau_{or} = \sqrt{\frac{2}{3}} \frac{GB}{W_{[001]}}$ contribution has been added to account for the structural hardening brought by the γ'-phase, whatever its kind of population (large or fine precipitation). G is the shear modulus ($= C_{44}$ for orthotropic materials, such as single crystal superalloys), B the Burgers vector magnitude ($= 0.254$ nm), and $W_{[001]}$ the γ-channel width along the [001] direction (i.e., in a (100) or a (010) plane). Since dislocations under high temperature conditions are mainly gliding in the matrix on octahedral slip systems, the $\sqrt{\frac{2}{3}}$ correction factor is added when calculating the Orowan stress, using γ corridor width along the [001] direction [24]. Linking $W_{[001]}$ with the volume fractions of large and fine γ' precipitates (see the next section) then enables the modeling of the γ' dissolution/precipitation effects upon the viscoplastic behavior.

- The second term of eq. (6) represents dislocation hardening through the isotropic state variable ρ^s and cross hardening by means of the interaction matrix [h]. For a given dislocation state, defined by a set of ρ^s on each slip system, the hardening consists of a steady-state contribution, given by Q, and a transient contribution, defined by Q^*. The material parameter Q depends on temperature only, while Q^* is a variable that depends on temperature and aging history (see further on).

$$r^s = \tau_0^s + b\left(Q + Q^*\right) \sum_j h_{sj} \rho^j + \sqrt{\frac{2}{3}} \frac{GB}{W_{[001]}} \quad (6)$$

$$\dot{\rho}^s = \left(1 - b\rho^s\right) \dot{v}^s \quad (7)$$

From a metallurgical point of view, eq. (6) can therefore be described as the sum of, from left to right, the solid solution hardening brought by the matrix ( ), the dislocation hardening and the structural hardening coming from the precipitates.

The evolution of the kinematic hardening x^S is classically defined on each slip system by means of the variable α^s(eq. (8)), which has a non-linear evolution with respect to the plastic slip on system s, γ^s (eq. (17)).

$$x^s = C\alpha^s \tag{8}$$

$$\dot{\alpha}^s = \left(sign\left(\tau^s - x^s\right) - d\alpha^s\right)\dot{\nu}^s \tag{9}$$

Microstructural evolutions considered

The main microstructure evolutions occurring during high temperature viscoplastic deformation of Ni-based single crystal superalloys are the γ / γ' morphological evolutions (i.e., homothetic coarsening, directional coarsening – so-called γ'-rafting [25-28]) and massive dissolution/re-precipitation processes occurring during temperature changes for a very high temperature domain (T ≥ 950°C). Figure 2 illustrates the γ / γ' morphological evolutions occurring during a high temperature/low stress creep test of a first generation Ni-based superalloy (MC2 alloy). The characterization of the γ / γ' morphological evolutions was performed by analyzing several interrupted creep tests at high temperatures and low applied stresses. These analyzes were devoted to identifying the evolution of $W_{[001]}$ as a function of time. Based on these observations, two different evolutions in the γ channel width $W_{[001]}$ were found, one mainly related to the γ' volume fractions of the different classes of γ' particles [12] (described further on) and one sensitive to the time-temperature-strain rate history [14, 15].

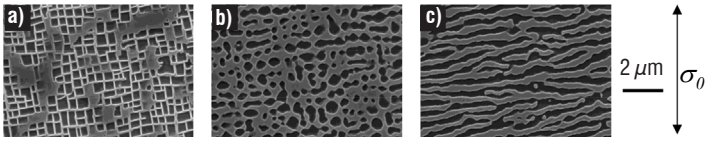

Figure 2 - γ' rafting during a creep test at 1050°C/160 MPa of MC2 alloy: γ / γ' microstructure at the beginning of the experiment (a), after 4.7 h (during primary creep stage) (b) and after 9.4 h (beginning of secondary creep stage) (c). Note that the γ' phase appears as dark areas

The precipitation evolution considered in the Polystar model are the γ' dissolution/precipitation mechanisms occurring during heating/cooling stages in a temperature range inducing pronounced γ' dissolution (T > 950°C for a majority of commercial alloys). Figure 3 illustrates what is happening for a single overheating close to the γ'-solvus of the alloy and figure 4 is an actual γ / γ' microstructure observation after an overheating.

As shown in figure 3, a fast γ' dissolution occurs during a temperature jump in the γ' dissolution domain, leading to a widening of the γ matrix channels (i.e., an increase in), i.e., to an easier viscoplastic flow due to the decrease in the Orowan stress. Such a γ' dissolution mechanism is accompanied by a decrease in the dislocation density at the γ / γ' interfaces, as shown by TEM observations [1] and more recently using in situ non-isothermal creep experiments followed by X-Ray diffraction (XRD) under synchrotron radiation [29, 30]. Cooling down to the nominal temperature entails the precipitation of hyperfine (tertiary) γ' particles in the γ channels, as well as an increase in the dislocation density at the γ / γ' interfaces (see the last column in figure 3). It means that the γ' precipitation during non-isothermal loading is no longer monomodal, but, at least, bi-modal, with two classes of γ' precipitate, as shown in figure 4. The respective volume fractions of coarse and fine (tertiary) γ' precipitates will be denoted as fl and fs in the rest of the paper. It is also worth mentioning that all of the microstructure evolutions occurring during very high temperature changes are highly dependent on the temperature levels, heating/cooling rates and durations of the overheating. Indeed, the microstructure of the material is left out of thermodynamical equilibrium if the temperature changes and the dwell times are respectively fast and short enough, hence leading to transient mechanical responses of the alloy (the new primary creep shown in the second column of figure 3 is a typical illustration of such a transient creep behavior). The microstructure evolutions presented in figure 3 are all taken into account in the Polystar model and their evolution laws are now presented.

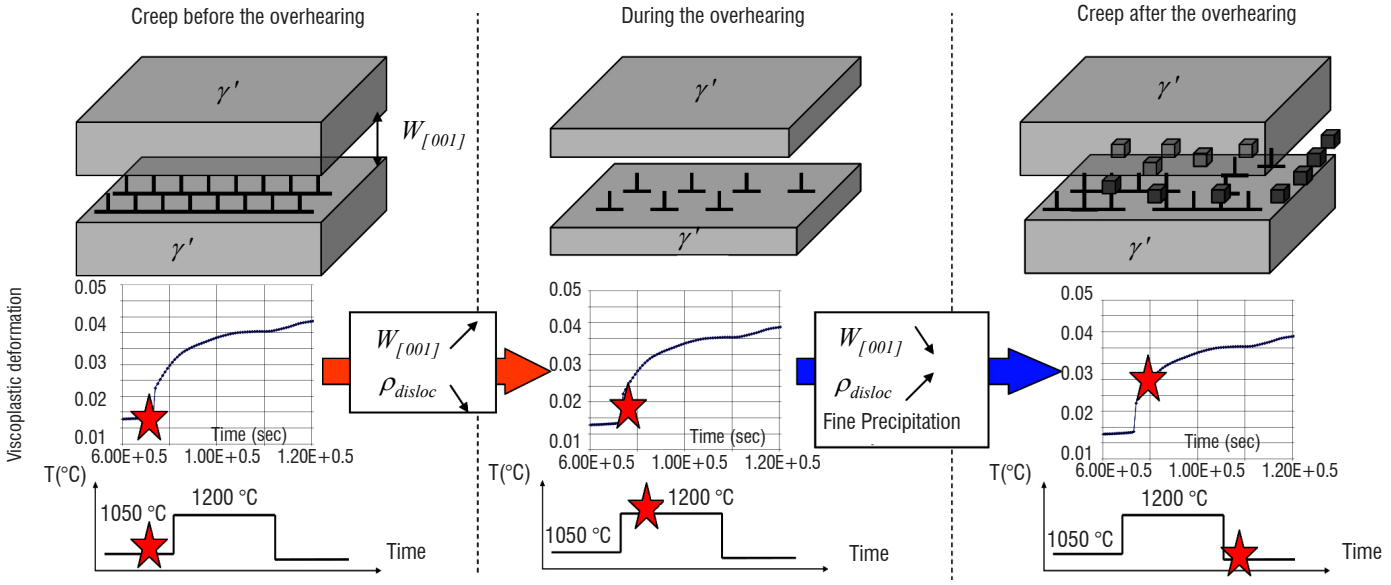

Figure 3 - γ' dissolution/precipitation mechanisms during a single overheating introduced after a given amount of creep deformation. The upper row is a schematic illustration of the γ / γ' microstructure and of the dislocation density evolutions. The middle row shows the evolution of the creep strain and the last row shows the actual position (red star) in the thermal history.

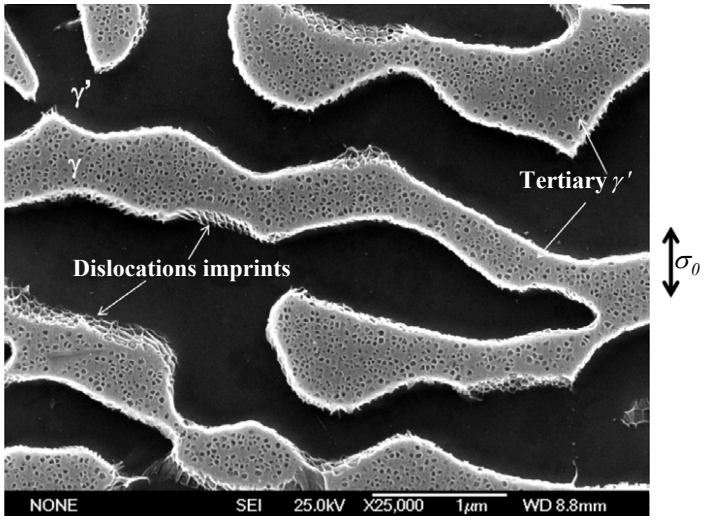

Figure 4 - γ / γ' microstructure obtained after a non-isothermal creep test performed with the CMSX-4 Plus® Mod C single crystal superalloy. The experiment was interrupted after an 1150°C overheating. Note ultrafine (tertiary) γ' precipitates in the γ channels. The γ' phase appears as dark areas.

An exponential type expression has been initially chosen to describe the evolution of the volume fraction of large γ' particles (f_l), as observed in IN100 polycrystalline superalloy [31], or more recently in MC2 alloy [19]. The same kind of evolution was chosen in recent phase field simulations performed by Wang et al to analyze the effect of the initial γ' precipitate size on dissolution kinetics [32]. α_l is the time constant for the dissolution/coalescence process depending on temperature. The temperature-dependent values of α_l and f_{equ} (the γ'-volume fraction at thermodynamical equilibrium) were measured from microstructural investigations performed previously [2, 19, 33].

$$\dot{f}_l = \frac{f_{equ} - f_l}{\alpha_l} \tag{10}$$

However, to obtain a better description of the dissolution/precipitation kinetics of large γ' particles, a modification of eq. (10) has been recently proposed. In fact, an impact of the accumulated plastic deformation on the dissolution kinetics was clearly demonstrated by Giraud et al. for CMSX-4® alloy [21]. Equation 10 was then modified into eq. (11), with and ecfl being temperature-dependent material parameters:

$$\dot{f}_l = \left[1 - \delta_l \times exp\left(-\frac{v}{e_{cfl}}\right)\right]\left(\frac{f_{equ} - f_l}{\alpha_l}\right) \tag{11}$$

A challenging issue was also to model the evolution of the fine γ' precipitation occurring in the γ channels on cooling (see figure 4). Indeed, it would have been easy to assume that $f_l + f_s = f_{equ}$, f_s being the volume fraction of small precipitates. Nevertheless, this equation is only valid when the tertiary precipitation occurs (cooling after a dissolution time). In fact, the small precipitates may not have the same chemical composition as the largest ones. It was even shown that the kinetics of dissolution or coalescence are different for large and small precipitates [33]. The following evolutions of the fine precipitate volume fractionare f_s then defined, considering isothermal conditions without overheating or during an overheating eq. (12), cooling after an overheating eq. (13) and re-heating after an overheating eq. (14):

$$\text{if } \left(f_{equ} - f_l\right) \le 0,\ \dot{f}_s = -\frac{f_s}{\alpha_s} \tag{12}$$

$$\text{if } \left(f_{equ} - f_l\right) > 0 \text{ and } \dot{T} < 0,$$

$$\dot{f}_s = -\frac{f_{equ} - f_l - f_s}{\alpha_s}\left(\frac{\dot{T}}{T_0}\right) - \left(\frac{f_s}{K_{s_1}}\right)^{m_s} \tag{13}$$

$$\text{if } \left(f_{equ} - f_l\right) > 0 \text{ and } \dot{T} \ge 0,\ \dot{f}_s = -\left(\frac{f_s}{K_{s_2}}\right)^{m_s} \tag{14}$$

Eq. (12) is a phenomenological representation of the dissolution of hyperfine precipitates during a temperature increase and during isothermal dwells. Under continuous cooling conditions after an overheating, both nucleation and dissolution have to be considered. Their respective contributions are taken into account by, respectively, the first and second terms in eq. (13) and both processes are highly dependent on the cooling rate. The last case occurs when the microstructure is out of equilibrium after an overheating (a population of hyperfine particles already nucleated) and a new overheating is occurring. Under such circumstances, a very fast dissolution of tertiary precipitates occurs (even faster than under the first case described by eq. (12)), which is taken into account by equation (14). The time constant α_s is smaller than α_l for the largest precipitates. In particular, the dissolution is quasi-instantaneous for temperatures over 1000 °C. Based on the γ' volume fraction evolutions presented in eqs. (11) to (14) and assuming that $W_{[001]}$ is only γ' volume fraction dependent, the following phenomenological dependence on f_l and f_s has been determined [12]:

$$W_{[001]} = \frac{a_0}{\delta}\left(f_l^{m_l} - d_{tp} f_s\right) \tag{15}$$

where a_0 is the initial average edge length of the γ' cubes (= 0.45 μm) and m_1, d_{tp} and δ are material parameters. This equation has been experimentally validated for both cuboidal and rafted γ' morphologies [12]. A linear dependence of $W_{[001]}$ on f_s has been introduced, since the fine precipitation filling the γ channels on cooling is very effective in narrowing them (the γ channel width can be as small as 10 nm). It should be admitted at this point of the study that the d_{tp} parameter has not yet been determined experimentally, due to difficulties in the stereological characterization of these ultrafine particles. It is also pointed out that an experimental evolution of $W_{[001]}$ on the γ' volume fractions has been chosen rather than physical models based on geometrical considerations [34, 35], since our model should take into account rapid changes of volume fraction under a wide range (from 0 to 0.7) and independently from the precipitate morphology (cuboidal or rafted). The authors also point out that eq. (15) is not able to capture slow morphological evolutions of the precipitates (i.e., γ' directional coarsening) under isothermal conditions. Indeed, this "medium version" of the model is suitable to the simulation of complex certification cycles of turboshaft engines for helicopters presented later in this paper. The durations of such thermomechanical histories (see, e.g., figure 10) are short enough to neglect the contribution of γ'-rafting to the viscoplastic behavior of the alloy. A more refined version of the model published last year takes into account such a time dependence of the γ' morphology of the precipitates [15].

The dislocation density evolutions occurring during temperature changes have been modeled through a decomposition of the work hardening (second term in eq. (6)): Q is a material parameter corresponding to the dislocation pinned at the γ/γ' interfaces, which cannot vanish during overheatings due to recovery processes (dislocation climb or γ'cutting/annihilation process), while Q^* is a variable describing the effect of microstructure changes on the dislocations density recovery. Q^*depends on a state variable a^* (eq. (16)) whose evolution range is [0,1]. Q_{S0} is then the maximum recoverable dislocation hardening. The evolution of a^* is presented in eq. (17): the metallurgical steady-state (maximum recovery) is obtained for $a^*=0$. The first term of eq. (17) accounts for the recovery effects upon temperature changes, while the second one represents the (re) establishment of dislocation structures after a temperature peak.α^* and β^* are the time constants for those processes with $\alpha^* << \beta^*$.

$$Q^* = a^* Q_{S0} \tag{16}$$

$$\dot{a}^* = -\frac{a^*}{\alpha^*}\frac{\dot{T}}{\dot{T}_0} - \frac{a^*}{\beta^*} \qquad a^*(t=0)=1 \tag{17}$$

The Q^* term hence allows a partial recovery of the isotropic hardening, due to thermal changes. The evolution of Q_{S0} as a function of temperature typically allows such recovery processes only at very high temperatures (T > 1100°C).

Damage law

Past non-isothermal creep tests with one single overheating performed on MC2 alloy showed that increasing the overheating duration led to increased creep life [1-3], while a stress-driven damage evolution would have predicted the opposite, since the applied stress remains almost constant. A plasticity driven damage evolution is hence proposed. The damage evolution is formulated at a microscopic level, on each slip system (eq. (18)). This damage evolution has been given a Rabotnov – Kachanov formulation [36]. Nevertheless, instead of using the applied stress, a kinematic variable $|x_d^s|$ is chosen as the critical variable. The use of x_d^s instead of $\tau^s$is motivated by the fact that a high frequency fatigue loading must not generate creep damage. This is naturally verified if x_d^s is the critical variable, since the plastic strain amplitude remains negligible and so does x_d^s. After a nucleation period defined by a threshold v_d (the accumulated viscoplastic strain must reach a given value $v > v_d$ before damage starts), the damage rate is defined as a power function of $\frac{|x_d^s|}{(1-d_c^s)}$, which produces a catastrophic softening and tertiary creep on a macroscopic level (eq. (18)).

$$\text{if } v > v_d,\ \dot{d}_c^s = \left(\frac{|x_d^s|}{K_x(1-d_c^s)}\right)^{m_x} \tag{18}$$

This evolution is somehow identical to previous models, where multiplication of mobile dislocations is a softening mechanism [37-39]. Pore growth is also a source of damage in this kind of alloys, but this is a relevant damage mechanism only in the last stage of life for which very steep tertiary creep occurs for creep strains greater than 5 % [40]. This would create a viscoplastic volume change that is not taken into account in our model.

Based on the experimental observations, the macroscopic creep strain threshold v_d beyond which the damage evolution is activated is typically between 0.5 and 1.5%, depending on the alloys and temperature. As for the viscoplastic behavior (eqs. (8) and (9)), the evolution of x_d^s is classically defined on each slip system by means of the variables x_d^s (eq. (19)), which have a non-linear evolution with respect to the plastic slip on system , γ^s (eq. (20)).

$$x_d^s = C_d \alpha_d^s \tag{19}$$

$$\dot{\alpha}_d^s = \left(sign\left(\tau^s - x_d^s\right) - d_d \alpha_d^s\right)\dot{v}^s - M\left|\alpha_d^s\right|^{m_s} \tag{20}$$

A static recovery term $-M|\alpha_d^s|^{m_s}$has been added in eq. (20) to allow better predictions of progressive tertiary creep stages. The evolution of this backstress is different for the one presented in eqs. (8) and (9), since the damage kinetics under both isothermal and complex thermal cycling conditions cannot be reproduced using x^s. Such a phenomenological formulation has indeed been shown to take into account in a reasonable way the effect of the thermal cycling frequency on the non-isothermal creep life (not shown here). A further improved version of the damage evolution has been recently used by Ghighi et al to account for long tertiary creep stages at low temperatures/medium to high applied stresses [13].

Identification of the model

Three different versions of the Polystar model exist, with different degrees of refinement. The version of the model presented in this paper, which can be qualified as the “medium version”, has been identified for two alloys (MC2 and CMSX-4®) in the 750 °C-1300 °C temperature range, while only the microstructural part was identified for AM1 alloy. This version of the model only considers γ' volume fraction evolutions and recovery processes during complex thermomechanical histories. The most refined version of the model, which takes into account morphological evolutions of the precipitates (such as γ' rafting) in addition to the microstructure evolutions already taken into account in the medium version of the model, was identified only for MC2 alloy in the 950 °C – 1200 °C temperature range. The less refined version of the model is almost identical to the medium version of the model, without considering kinematic hardening (eqs. (8) and (9)) and static recovery in the damage evolution. It also neglects the coupling between the accumulated creep strain and the dissolution kinetics of the γ' phase (i.e., eq. (10) is used instead of eq. (11)). It is hence only useful for the modeling of the uniaxial creep behavior without a better numerical efficiency. The simplest version requires 28 material parameters (9 of these directly given by microstructure characterizations) to be identified per temperature [12], the medium one (the one presented here) requires 36 parameters per temperature (11 of these given by microstructure analyzes) while the most complex one requires 45 parameters to be identified (17 of these given by microstructure analyzes) [15]. Among all of these parameters, those characterizing the microstructure evolutions can be determined separately through microstructure investigations and specific XRD experiments detailed hereafter.

In the rest of the paper, all of the simulations presented in the figures result from the use of the medium version of the model, except

in figure 14 where the most refined version of the model has been used. It has been chosen not to detail this refined version in this article, since this most refined model has been identified in a narrower temperature domain (and it is not applicable to large temperature variations like the ones presented in figures. 11 and 15. The interested reader is referred to le Graverend et al for further details [15].

Microstructure evolutions

The identification of the dissolution/precipitation kinetics of the γ' phase is typically performed using heat treatments and subsequent image analysis techniques [41]. This procedure has been used several times for MC2 and CMSX-4® alloys in the past [12, 19, 42]. figure 5 illustrates such a direct identification of eq. (11) using several short thermal treatments at 1250°C after different amplitudes of creep deformation (in the 0% - 0.5% range) introduced at high temperature (1050°C in the case presented in figure 5). The γ' volume fraction at equilibrium (at 1250 °C here) can be directly determined by using the horizontal asymptote, while the other parameters of eq. (11) (e_{cfl} , δ_1 and α_1) are determined through an inverse method.

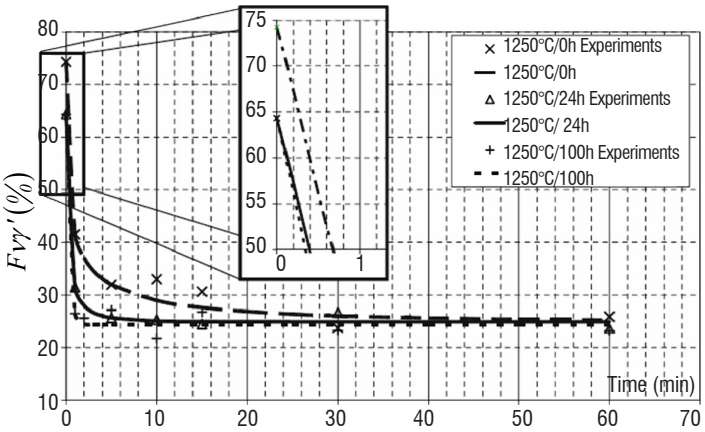

Figure 5. γ' volume fraction evolution in CMSX-4® as a function of the dwell time at 1250 °C without and with a prior creep deformation at 1050°C of 24 hours and 100 hours [42].

Despite the robustness of this method, it has to be reproduced for various temperatures of interest in the γ' dissolution domain (typically above 950 °C, by 50 °C steps) and this method is hence very time consuming. In addition, the fundamental assumption of such a method is that the microstructure evolutions, likely to occur during heating and cooling from/to room temperature, do not affect the microstructure obtained at the end of the heat treatment before final cooling. More recently, a new method has been proposed in close collaboration with Institut Jean Lamour / *Ecole des Mines de Nancy* to calibrate the equations accounting for the γ' volume fraction evolutions. It consists in a quasi-continuous monitoring of the actual γ' volume fraction during a non-isothermal creep test, using XRD characterizations under a synchrotron beam [43]. With such a method, uncertainties in microstructure characterizations due to heating/cooling to room temperature are suppressed. This method has been used for AM1 and CMSX-4® alloys and it is illustrated in figure 6 for AM1 alloy [29, 30, 44]. A very good modeling of the experimental evolution of the large γ' volume fraction (f_1) using the Polystar model is observed in figure 6. Hence, by varying the temperatures reached during overheatings, the heating/cooling rates and the positions of temperature changes in the creep life of the alloy (i.e., the amount of creep deformation), all of the material constants presented in eqs. (11) to (14) can be identified using at the most two to three experiments.

Mechanical behavior and damage law

The material parameters governing the mechanical behavior and the damage evolution have been identified on a large database composed of both isothermal experiments (tensile, low cycle fatigue and creep tests) and non-isothermal creep tests mainly performed on [001] oriented samples. An optimization process using the optimizer module *Z-opt* of the ZéBuLoN software suite [45] was performed to identify the flow rule parameters (n,K), as well as $\tau_0^S, b; C, d$ and $(Q+Q_{S0})$. These parameters were identified from a set of tension tests at high temperatures with different strain rates (typically, 1.10^{-3} s^{-1}, 1.10^{-4} s^{-1}, 1.10^{-5} s^{-1}), LCF tests with various strain amplitudes (two to three tests) and at least four isothermal creep experiments per temperature. Subsequently, non-isothermal creep experiments with various single overheating lengths and positions in the isothermal creep life under a high temperature/low stress condition were carried out to identify $a^*, \alpha^*, b^*, and\ \beta^*$. The experiments used for the identifications were chosen so that the temperature jumps were always performed once a rafted microstructure had been generated before the overheating. The damage evolution parameters $(K_X, C_d, D_d, M, m_x, m_s)$ were manually identified from both isothermal and non-isothermal creep tests using the same procedure.

Figure 7 illustrates the model predictions of the non-isothermal creep behavior and durability of the first generation Ni-based single crystal superalloy MC2. Various overheatings close to the γ' solvus of the alloy (overheatings at 1200°C in figure 7) were introduced somewhere in the creep life of the alloy at 1050°C/140 MPa using the burner rig Thalie developed at Institut Pprime [5]. Very good performances of the model are observed, both in terms of elongation and creep life. Indeed, as observed in figure 7, all of the creep stages are properly taken into account, including the new primary creep stage after the overheating and the change in creep strain rate after the overheating resulting from the microstructure evolutions during the overheating.

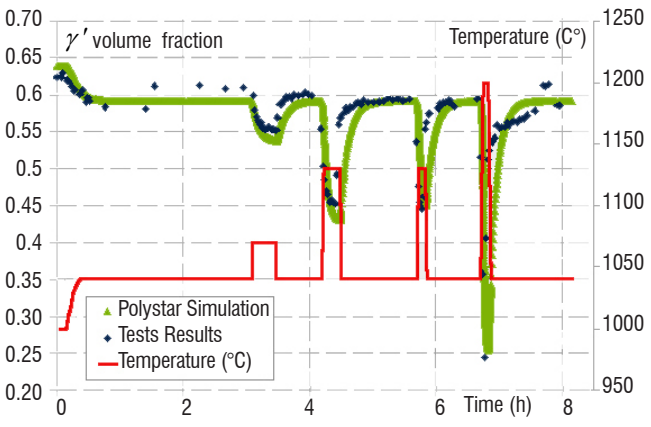

Figure 6 - γ' volume fraction evolution in AM1 alloy (blue dots) as a function of time for a complex non-isothermal creep test [29]. The temperature history appears in red and the model simulation is represented by the green continuous line. The applied stress maintained constant during this experiment.

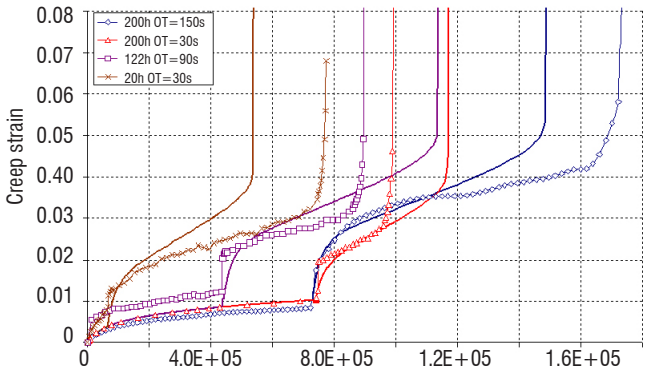

Figure 7 - Comparison between Polystar simulations (continuous curves) and experimental creep elongations (dotted curves) during non-isothermal creep experiments using MC2 alloy [1, 2]. These experiments included a single overheating at 1200 °C of different durations (OT = Overheating Time) ranging from 30 to 150 seconds, introduced somewhere in the creep life at 1050 °C/140 MPa of the alloy. Note that the actual positions of the overheating are included in the legend.

Complex thermomechanical history simulations and industrial applications

Presentation of the MAATRE burner

The evaluation of the Polystar model performances has been performed using very complex thermomechanical histories characteristic of those encountered by the high pressure turbine blades of turboshaft engines in helicopters during certification procedures. As has already been mentioned in the introduction, such procedures consist of a mixture of different engine regimes, including repeated over-temperature events. The use of classical laboratory test benches has already been shown to be excessively conservative (i.e., too low creep lives, too high amount of creep elongation during overheatings) to be representative of the in-service mechanical behavior of Ni-based single crystal superalloys during these events, since heating/cooling rates with a good temperature control are usually too slow [5]. Hence, 150h or ASMET engine tests have been reproduced using a very unique burner rig (the MAATRE burner) developed at Institut Pprime. A schematic illustration of its working principle is shown in figure 8.

As observed in figure 8, a burner based on the combustion of natural gas with air supplies hot gases that are blown onto the sample lying in the testing section. To reach higher temperatures for some very

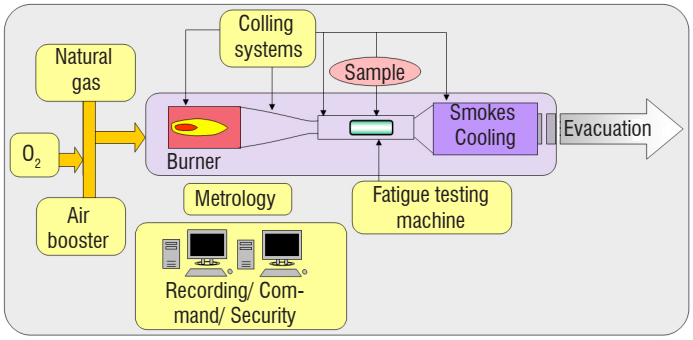

Figure 8 - Working principle of the MAATRE test bench

specific conditions, the combustion could be doped with oxygen. These hot gases are accelerated using a convergent located in the exhaust section of the burner, hence allowing a sufficient gas velocity in the testing section and a subsequently high heat exchange at the sample surface to allow very fast heating and cooling rates. Samples are also mechanically loaded (under monotonic or cyclic loading paths) with an electromechanic testing machine or a creep frame and they could be internally cooled by compressed air. Monitoring and controlling all of these equipment parameters (gas and sample temperatures, gas flow, cooling flow and temperatures, sample displacements, applied load of the sample, etc.) as well as managing security are ensured using a central computer. Gas temperatures up to 1650°C can be reached in the testing section, with hot gas velocities up to 400 m.s-1. Controlled heating/cooling rates as high as 150°C/s can be obtained within this equipment, which is essential for the engine tests presented in this paper. The mechanical loading, during the tests presented in this article, was applied with a creep testing machine using dead weights. An illustration of the test bench equipped with this creep testing machine is presented in figure 9.

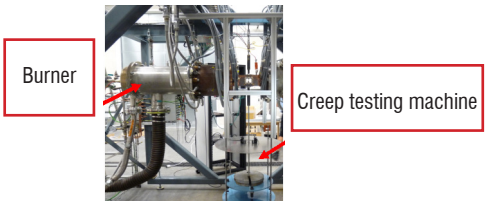

Figure 9 - MAATRE test bench equipped with the creep testing machine

A specific metrology has been developed for measuring both the displacement and temperature of the sample, in order to perform accurate interpretations of the tests. During the subsequently presented tests, the temperature of the sample was measured with a spot welded S type thermocouple. The diameter of this thermocouple must be large enough to ensure a sufficient mechanical resistance to the aerothermal drag generated by the hot gas flow and small enough to avoid thermal perturbations from the thermocouple wire. A 0.35 mm in diameter thermocouple was used. The combustion in the burner section was directly controlled with a closed loop using this temperature measurement. During experiments, elastic, thermal and creep strain were measured using a videoextensometry technique. Strain measurements are performed using markers deposited in the central part of the gage length of the samples, where the temperature is spatially homogeneous (with a +/-3°C accuracy). The interested reader is referred to two previous papers from the authors for further details [4, 16].

Testing conditions

Two kinds of engine tests were performed, namely a “150h” and “ASMET” (Accelerated Simulated Mission Endurance Testing). These tests comprise different stages. These stages can be divided into “long term” temperature steps or successive temperature peaks. The details of these testing conditions are presented in figure 10.

A tensile stress is applied to the specimen during the test. It is worth mentioning here that overheatings around 1220 and 1240 °C are very close to the γ'-solvus (Tsolvus = 1265 °C) of the alloy used for this study, namely, the first generation MC2 alloy [12, 19].

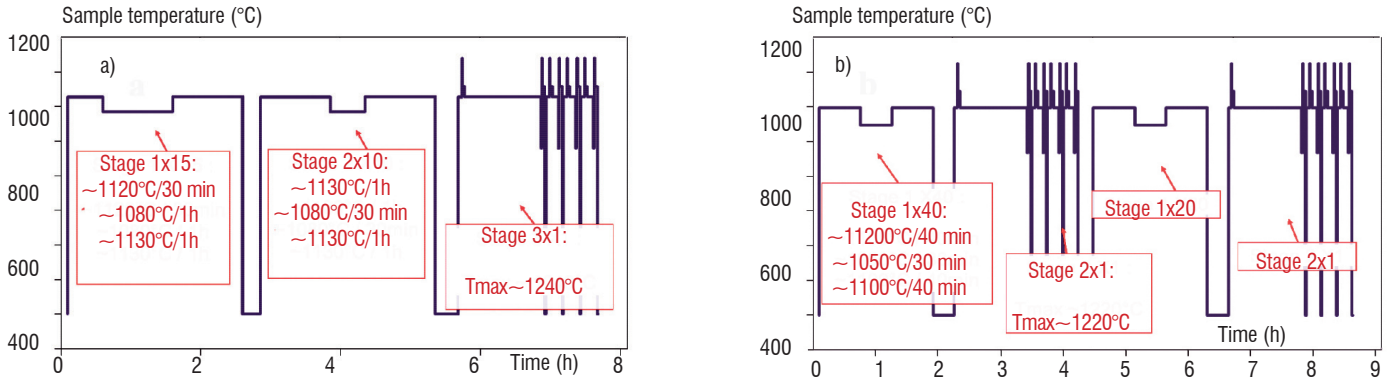

Figure 10 - Testing conditions for the 150h test (a) and the ASMET test (b)

Experimental results and performances of the Polystar model

The evolutions of the viscoplastic strain and measured temperature as a function of time are given in figure 11 for both the ASMET and 150h tests. Under such conditions of strain measurements for a sample loaded under the impact of a gas flow, the creep strain measurement can be considered to be very satisfying. It must be pointed out that the absence of strain measurements between 75 and 100h for the ASMET test (figure 11b) is due to a computer data overflow. According to figure 11, a progressive decrease in the creep rate during the two first stages of the 150h test is observed (figure 11a), and, as expected, a steep increase in the creep rate during the last stage containing the overheatings. Indeed, each temperature peak involves a fast creep strain jump. This fast increase in the strain rate has also been observed in [4]. The ASMET test is less damaging than the 150h one, based on a creep strain criteria (figure 11b). In addition, the creep strain increase during the overheatings is less pronounced compared to that observed during the overheatings of the 150h test. This is consistent with the fact that the overheatings performed during the 150h test are closer to the γ'-solvus of MC2 alloy (see figure 10).

The Polystar performances have been evaluated using these complex experiments performed under combustion environment. The simulations have been performed considering a homogeneous spatial distribution of the temperature at each time. Using such an assumption, a simulation at one Gaussian point can be directly compared to the experimental result. A rather good agreement between the experimental result and the simulation can be observed in figure 12. In addition, it is observed that the model predicts in a reasonable way the creep strain jumps entailed by the overtemperatures. This is more clearly observed in figure 13, where it is observed that the calculated jumps' amplitude is increasing while, experimentally, the amplitude of the creep strain jumps remains almost constant. This difference results from a non-negligible damage increase in the model while, according to microstructural observations performed elsewhere, only limited evidences of creep damage in the form of deformation pores and submicron crack initiation at casting pores were observed [4]. According to the simulation, the material should have failed a few minutes before the end of the test.

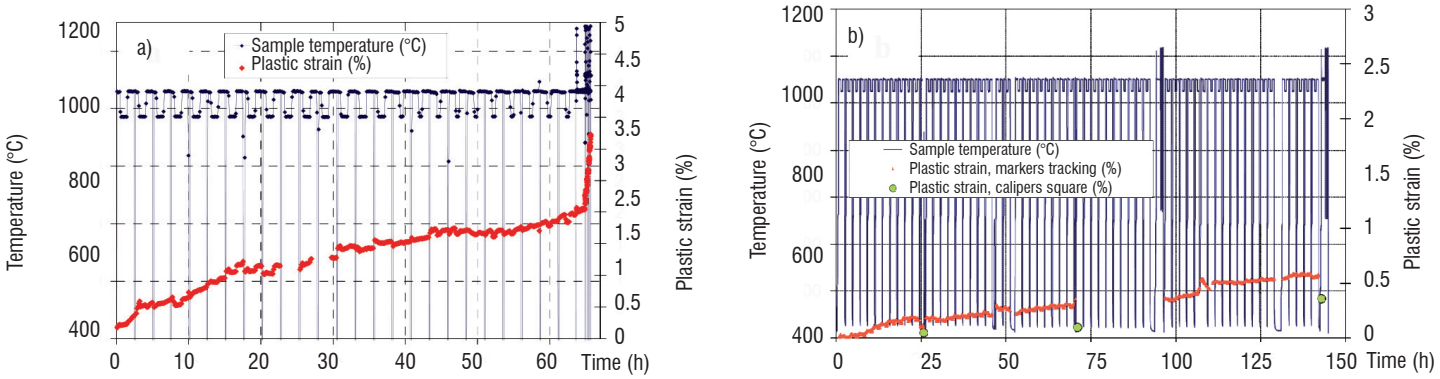

Figure 11 - Evolution of plastic strain (red curves) and sample temperature (blue curves) as a function of time for the 150h (a) and ASMET (b) tests.

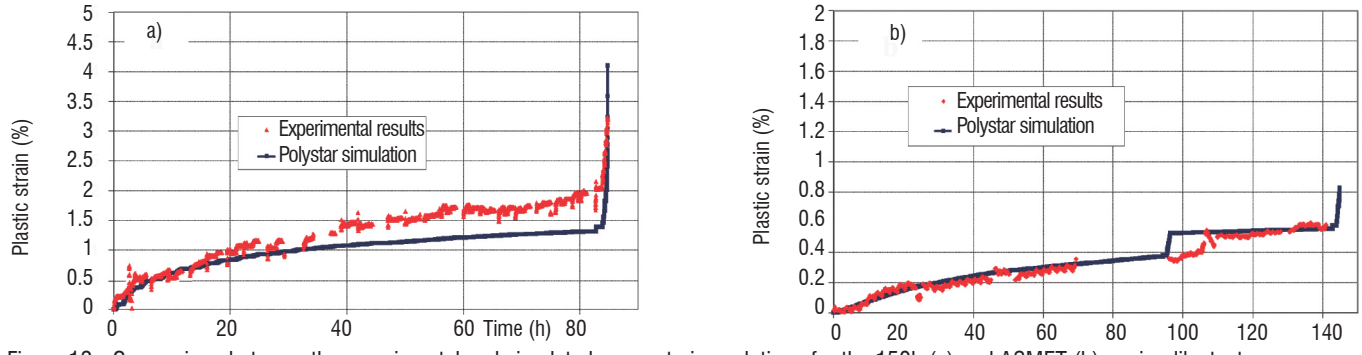

Figure 12 - Comparison between the experimental and simulated creep strain evolutions for the 150h (a) and ASMET (b) engine-like tests.

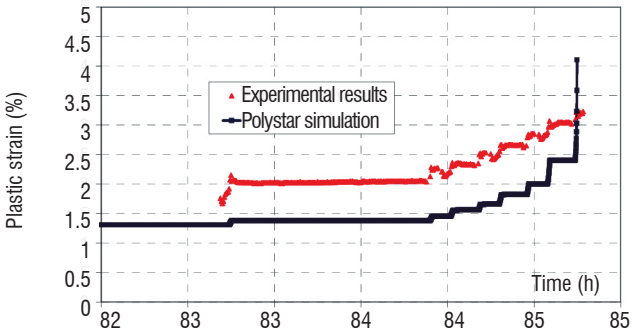

Figure 13 - Comparison between the experimental and simulated creep strain evolutions for the 150h engine-like test during the last stage.

Evaluation of the model under complex mechanical field and industrial applications

The two simulations presented in the previous section showed the Polystar capabilities for estimating the plastic strain monitored during complex tests representative of in-service thermomechanical conditions. The model seems to be very accurate in the lowest temperature range of testing, but it can overestimate the creep strains in the highest ones (T > 1200 °C). This may come from a poorer precision in the model calibration at very high temperature levels. Nevertheless, this model with its additional internal variable is the only one able to capture complex microstructural phenomena, such as dissolution/precipitation of strengthening particles, dislocation recovery processes and their impact on the mechanical behavior. Under very intricate conditions, such as those presented in this article, this model performs better than any other model where the temperature dependence is only taken into account through the temperature dependence of the material coefficients.

As a further evaluation of the model performances, a complex non-isothermal experiment using a bi-notched specimen has been used and compared to a 3D finite element simulation using the Polystar model as a constitutive material behavior. The sample geometry can be observed in figure 14. This experiment under constant

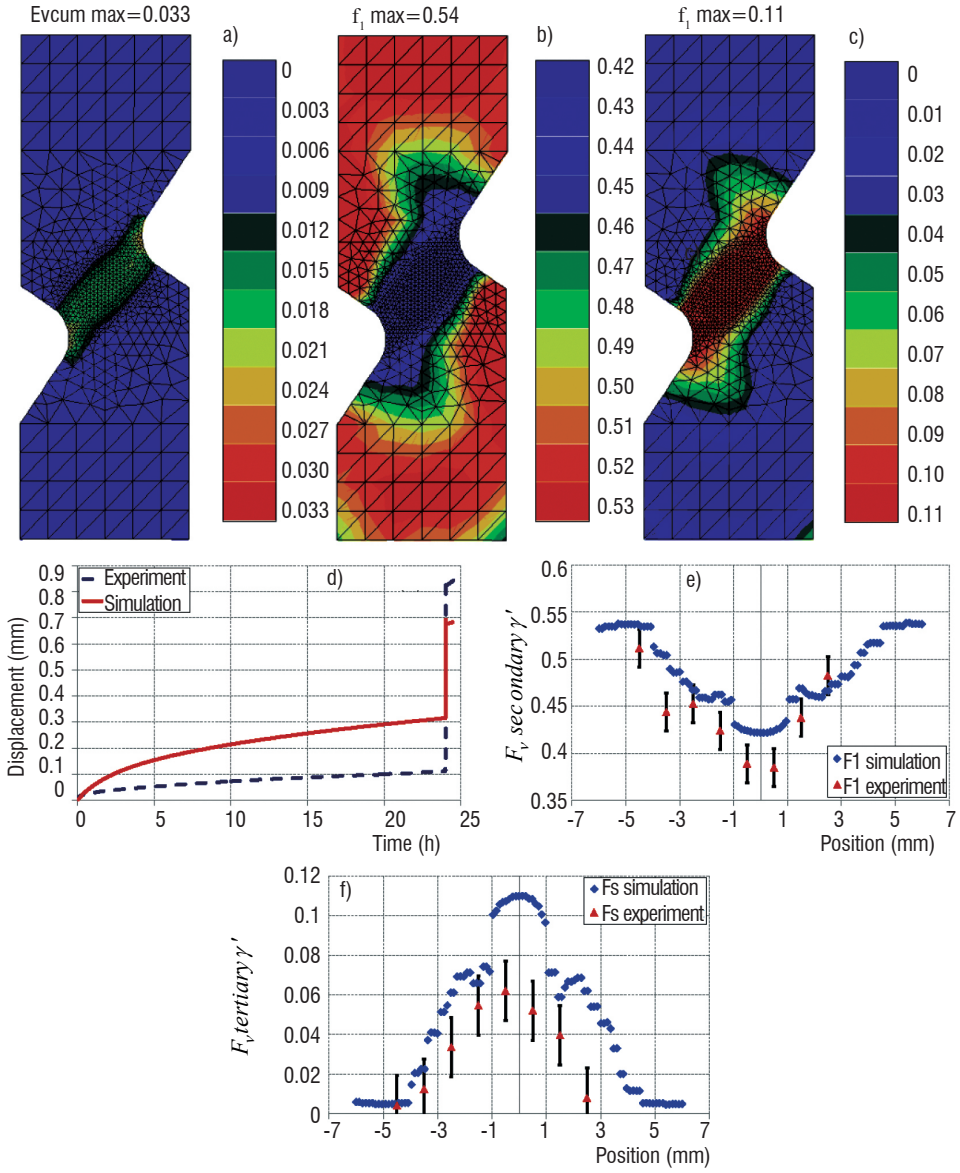

Figure 14 - Prediction of (a) the accumulated plastic strain (ν or evcum), (b) the volume fraction of secondary γ' precipitates (f_1) and (c) the volume fraction of tertiary γ' precipitates (f_s). (d) Comparison between the elongation predicted by the model and the experimental elongation. (e) and (f) correspond respectively to the evolution of the volume fractions of secondary and tertiary γ' precipitates presented in (b) and (c) along a vertical central path shown in (a).

load consists of 24h at 1050 °C, followed by a short temperature spike of 20 seconds at 1200 °C and 30 additional minutes at 1050 °C after the overheating. After testing, microstructure observations were done and volume fraction measurements of secondary (f_l) and tertiary $(f_l)\,\gamma'$ precipitates were performed. Further details about this experiment can be found in [15].

As expected, a greater creep strain at the end of the test is predicted between the two notches (figure 14a). Such a difference in local creep strain greatly affects the evolutions of secondary and tertiary γ' particles. This effect is properly considered by the model (figures. 14a and 14b respectively for fl and fs) through eqs. 11 and 12 to 14. Comparing γ' volume fraction measurements with the simulation along the path defined in figure 14a, a good agreement is observed (figures. 14e and 14f), despite huge difficulties in the experimental characterization of the tertiary γ' evolutions (dissolution/precipitation) [12]. A comparison between the longitudinal creep displacement (along the vertical in figure 14a) monitored during the experiment and the computed one has also been performed. A quite pronounced difference is observed in figure 14d, both during the isothermal part before the overheating and during the overheating itself. Indeed, an overestimation of the creep elongation by the model is observed before the overheating and an underestimation of the creep accumulation is observed during the overheating. Such differences were partly attributed to crystal lattice rotations, where the multi-axial state of stresses are the largest [15].

After such laboratory evaluations/validations of the model under complex thermomechanical histories using smooth specimens or notched ones (technological samples), the model has been introduced in the SAFRAN – Turbomeca Methods Department. The model performances are presently evaluated at Turbomeca using 1D beam-like calculations, each slice of the beam being assigned the spatial average stress and temperature histories of one section of an HP blade profile. Moreover, 3D finite element simulations using Z-Ansys as software and the Polystar model have been performed. A complex thermomechanical history (presented at the bottom of figure 15) representative of a certification test has been chosen as an input loading. Figure 15 shows the evolution of the von Mises stress, of the accumulated creep strain (v) and of the secondary γ' volume fraction (fl) distributions in an HP blade profile after one, five and ten missions. It is observed in this figure that the hottest areas close to the leading edge, where the γ' volume fraction turns to blue, do not correspond necessarily to the most severely creep-deformed areas. In addition, it is observed that even if the von Mises stress distribution hardly evolves, a creep strain accumulation is observed and an even lower γ' volume fraction at the leading edge is obtained thus increasing the mission number, due to a higher creep strain, which accelerates the γ' dissolution (see eq. 11). Such calculations are presently used to predict the elongation and the durability of HP blades during complex certification engine tests. It is especially useful to evaluate the safety margins that can be used during the certification of new turboshaft engines for helicopters. According to Turbomeca practices, this model may also reduce the design durations/costs with a closer-to-reality prediction of the creep behavior (in terms of elongation and durability) of an HP blade made of Ni-based single crystal superalloys.

Limitations of the model, on-going activities and additional potential use

According to various previous studies, several limitations listed hereafter were already observed in the model:

• A poor description of the cyclic ratcheting was observed by le Graverend [46] under uniaxial high temperature dwell-fatigue conditions. No solution has been found up to now and one possible solution would be the introduction of a second kinematic hardening term in the yield function in the octahedral slip systems.

• The model was observed to provide poor predictions of the elongation/shear strain under isothermal and non-isothermal multiaxial loadings (e.g., tension-torsion tests using single crystalline tubes, tension tests on notched samples) [46]. This was especially observed when large shear stresses were introduced. Figure 14d is a good illustration of this. Some on-going investigations by A. Mattiello in the context of a collaboration between LMT Cachan, SAFRAN – Turbomeca and Institut Pprime are devoted to the formulation of the model in a large strain context, to account for the crystal lattice rotations observed under such conditions [47]. In addition, a better identification of the interaction matrix between slip systems and the introduction of cube slips will further be evaluated. Taking into account lattice rotations should also allow a better modeling of the tertiary creep stages when considering the tensile creep acceleration for misoriented samples [12, 13].

• Even if the model was initially devoted to the modeling of very high temperature (T > 1000 °C) non-isothermal creep conditions, low temperature creep under a large applied stress condition remains a critical issue for cooled components, especially in the web sections [48, 49]. Under such conditions, the <112>{111} slip activity has to be considered for various alloys, since it can contribute to large primary creep strains of up to 10 pcts [49]. The associated question is how the identification of the materials parameters characterizing such a slip activity on <112>{111} systems must be done, since the slip activity on these systems results from a classical <110>{111} slip activity (i.e., both slip systems are co-existent) and is highly dependent on the crystal orientation and applied stress. This work is presently in progress for the case of CMSX-4® alloy [47].

• Finally, due to the large number of internal variables introduced in the model, computation times are rather long, especially for industrial perspectives. A reduced model (i.e., suppressing some second-order internal variables) or more efficient calculation schemes must be made.

In regard to the potential additional uses of the model, it has been shown in the previous sections that the Polystar model provides good evaluations of the microstructure evolutions, especially in terms of secondary γ' precipitate volume fraction f_l (see for example figures 6 and 14). In addition to the computation of the mechanical behavior and durability of Ni-based single crystal superalloys used for the components of the hot sections of gas turbines, the microstructure module of the model can also be used as an

expert assessment tool for the estimation of local metal temperature histories. Indeed, knowing the T41 temperature evolution in an engine (T41 being the gas temperature at the exhaust of the combustion chamber), the resulting true metal temperature history can be computed by an inverse method, using a final microstructure inspection of a component. This microstructure part of the model can even be considered as a potential tool for validating thermal calculation methodologies used in design departments.

Finally, since the model is sensitive to some initial microstructure features, such as the γ' size or the γ' volume fraction at thermodynamical equilibrium, this model is also, by nature, sensitive to some microstructural differences from the "standard state" likely to result from the elaboration processes. As an example, an evaluation of the impact of a small variation in the as-received γ' content on the mechanical response can be done easily with this model, as has already been shown in the pioneering paper on this model [12]. A more systematic study would be required to obtain a good estimation of scatter bands around the average mechanical behavior resulting from such small variations of the parameters representing the initial microstructure. All of this work remains, however, to be done.

Concluding remarks

A microstructure sensitive model (the Polystar model) has been developed within the framework of crystal plasticity, in order to be predictive of the non-isothermal viscoplastic behavior of Ni-based single crystal superalloys, especially when rapid microstructure evolutions are likely to occur, such as γ' strengthening phase dissolution, dislocation recovery processes, or hyperfine precipitation in the γ matrix. Such rapid microstructure evolutions are encountered during the certification procedure of aeronautic gas turbines and they lead to transient mechanical behaviors that cannot be reproduced with standard constitutive modeling approaches without any additional internal variables. This model, mainly developed since 2007 at Institut Pprime – ISAE-ENSMA (among other partners), is based on the introduction of new internal variables, such as the γ' volume fraction of coarse

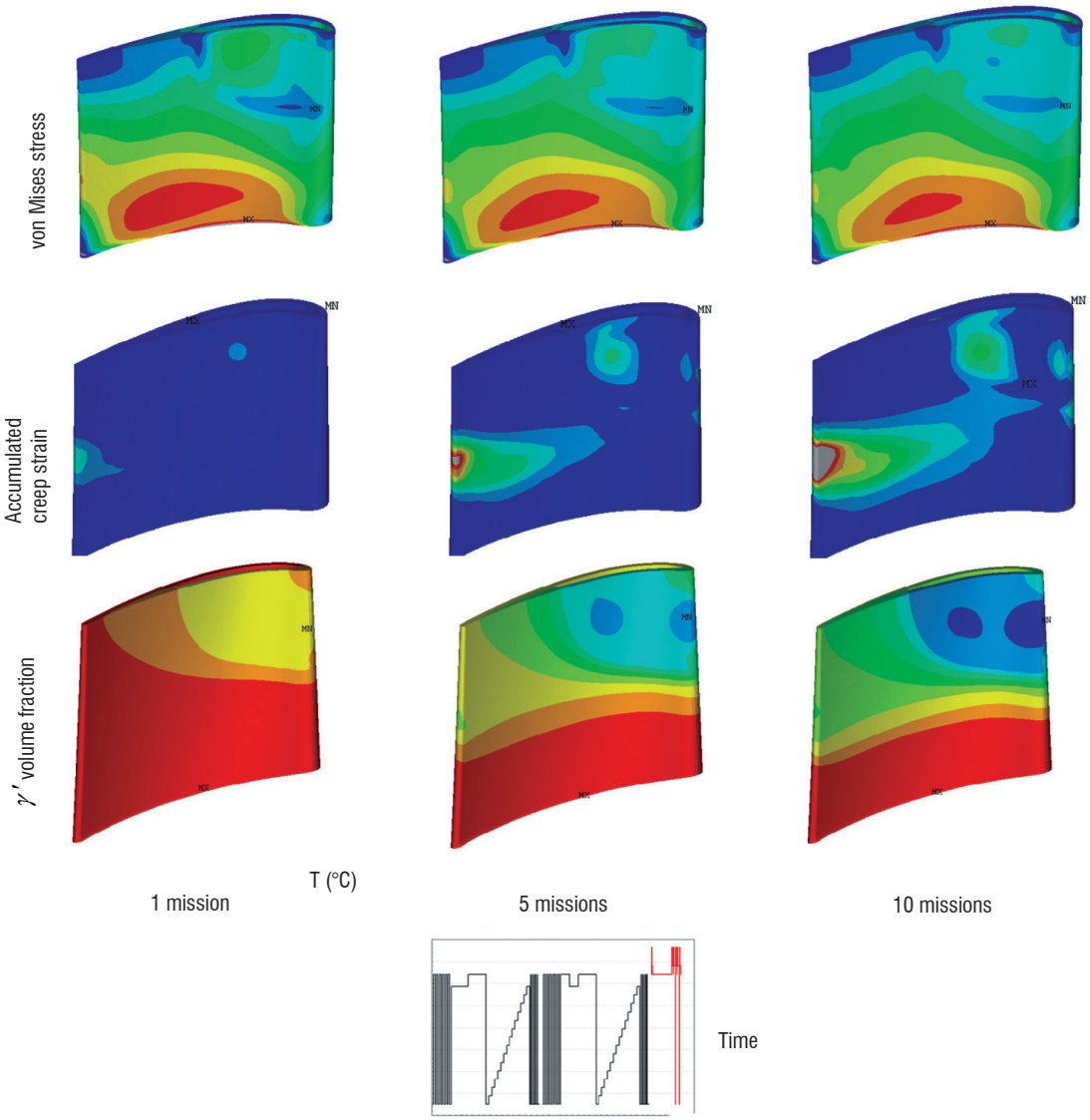

Figure 15 - Evolutions of the von Mises stress, of the accumulated creep strain (v) and of the γ' volume fraction (f_l) spatial distributions in an HP blade profile, as a function of the number of certification missions. The mission used for the simulation is presented at the bottom of this figure and is typical of a 150h engine test. Color code: higher von Mises stresses, higher accumulated creep strain and lower γ' volume fraction fl from blue to red.

and small particles or a temperature dependent aging variable, to account for dislocation recovery. Various versions of the model have been tailored with a more or less refined description of microstructure evolutions.

It is shown in this paper that the model provides good predictions of the non-isothermal viscoplastic behavior of Ni-based single crystal superalloys under complex thermomechanical loading histories. It is also shown that the identification and validation of this model can be improved and eased by the use of very specific experiments, such as in situ XRD creep experiments under a synchrotron beam to accurately evaluate microstructure evolutions, as well as by performing very unique experiments with fast heating and cooling rates up to extreme temperatures. Such unique experiments are recreated at Institut Pprime with the large scale facility MAATRE, a specific burner rig fully developed internally to be able to achieve representative testing conditions of the hottest sections of gas turbines, with an excellent metrology.

After the validation of the Polystar model in a laboratory context, this model has been implemented in the SAFRAN – Turbomeca lifing chain for a deeper evaluation within an industrial context in the Methods Department. Full-scale 3D calculations were successfully performed and, despite all of its remaining deficiencies presented in this paper, the Polystar model is the set of constitutive equations that provides the best estimations of the HP blade elongation and durability during engine certification procedures ■

Acknowledgements

Financial support from the French Ministry of Defense (DGA) and SAFRAN-Turbomeca is gratefully acknowledged. The authors are also grateful to SARGI S.A. for their help and efficiency in the design of the very unique burner used in MAATRE. The financial support from the CPER and FEDER (Poitou-Charentes Region, Vienne Department, European Community, Poitiers Agglomeration and French Education and Research Ministry) for the construction of MAATRE is also gratefully acknowledged.
JC, JM and FM are grateful to SAFRAN-Turbomeca for the continuous collaboration on superalloys for over 12 years: Dr. Elisabeth Ostoja-Kuczynski, Dr. Zéline Hervier, Dr. Antoine Organista, Dr. Sandrine Lesterlin and Dr. François Vogel are especially thanked for their continuous interest and encouragement. Former PhD students at Institut Pprime and SAFRAN-Turbomeca (Dr. Julien Ghighi and Dr. Rémi Giraud) who used the Polystar model and who participated to its development are also gratefully acknowledged for their contribution. Dr. Serge Kruch and Dr. Franck Gallerneau (ONERA/DMSM) are gratefully acknowledged for their help in improving the most refined version of the Polystar model. Dr. Alain Jacques, Dr. Thomas Schenk and Olivier Ferry (Institut Jean Lamour, Ecole des Mines de Nancy) are acknowledged for their valuable experimental contributions (XRD during non-isothermal creep experiments using a synchrotron beam) and for stimulating discussions. The Cannon Muskegon Corporation (Dr. Jacqui Wahl and Dr. Ken Harris) is gratefully acknowledged for providing several Ni-based single crystal samples. Stimulating discussions and exchanges with Dr. Farida Azzouz (Centres des Matériaux, MinesParistech) have been highly appreciated.
JC is indebted to Pr. Georges Cailletaud (Centres des Matériaux, Mines Paristech) who shared all of his experience in the pioneering developments of the Polystar model and for all of the stimulating discussions. Finally, JC is very grateful to Dr. Serge Kruch and Dr. Esteban Busso for their continuous encouragement in the preparation of this article

References

[1] J. CORMIER, X. MILHET and J. MENDEZ - Acta Materialia, 2007. 55(18): p. 6250-6259.
[2] J. CORMIER, J., X. MILHET, F. VOGEL, and J. MENDEZ - Superalloys 2008. Seven Springs, Champion, PA, USA.
[3] J.-B. LE GRAVEREND, , J. CORMIER, F. GALLERNEAU, S. KRUCH and J. MENDEZ - Materials and Design. 2014. 56(April): p. 990-997.
[4] F. MAUGET, D. MARCHAND, G. BENOIT, M. MORISSET, D. BERTHEAU, J. CORMIER, J. MENDEZ, Z. HERVIER, E. OSTOJA-KUCZYNSKI and C. MORICONI - Eurosuperalloys 2014. 2014. Presqu'île de Giens, France: Matec Web of Conferences.
[5] J. CORMIER, X. MILHET, J.-L. CHAMPION and J. MENDEZ - Advanced Engineering Materials. 2008. 10(1-2): p. 56-61.
[6] J. CORMIER, X. MILHET and J. MENDEZ - Materials Science and Engineering A, 2008. 483-484: p. 594-597.
[7] J.-B. LE GRAVEREND, J. CORMIER, M. JOUIAD, F. GALLERNEAU, P. PAULMIER and F. HAMON - Materials Science and Engineering, 2010. A527(20): p. 5295-5302.
[8] G. CAILLETAUD - 1979, Doctoral Thesis, University of Paris VI.
[9] G. CAILLETAUD and J.-L. CHABOCHE - Third International Conference on Mechanical Behaviour of Materials (ICM-3). 1979. Cambridge (G.B.): Pergamon Press.
[10] G. CAILLETAUD, J.P. CULIE and H. KACZMAREK - 1983. Stockholm: Tiré à part ONERA T.P. n° 1983-86.
[11] J. CORMIER and G. CAILLETAUD - Technische Mechanik, 2010. 30(1-3): p. 56-73.
[12] J. CORMIER and G. CAILLETAUD - Materials Science and Engineering, 2010. A527(23): p. 6300-6312.
[13] J. GHIGHI, J. CORMIER, E. OSTOJA-KUCZYNSKI, J. MENDEZ, G. CAILLETAUD and F. AZZOUZ - Technische Mechanik, 2012. 32(2-5): p. 205-220.
[14] J.-B. LE GRAVEREND, J. CORMIER, S. KRUCH, F. GALLERNEAU and J. MENDEZ - Advanced Materials Modelling for Structures H. Altenbach and S. Kruch, Editors. 2013, Springer. p. 189-199
[15] J.-B. LE GRAVEREND, J. CORMIER, F. GALLERNEAU, P. VILLECHAISE, S. KRUCH and J. MENDEZ - International Journal of Plasticity, 2014. 59: p. 55-83.
[16] F. MAUGET, F., D. MARCHAND, M. MORISSET, D. BERTHEAU, J. CORMIER and J. MENDEZ - Matériaux & Techniques, 2012. 6/7: p. 541-545.
[17] L. MÉRIC AND G. CAILLETAUD - Journal of Engineering Materials and Technologies, 1991. 113: p. 171-182.
[18] G. CAILLETAUD, J.-L. CHABOCHE, S. FOREST and L. RÉMY - La Revue de Métallurgie, 2003(Feburary): p. 165-172.
[19] J. CORMIER, J., X. MILHET and J. MENDEZ - Journal of Materials Science, 2007. 42(18): p. 7780-7786.
[20] J. CoRMIER, J., M. JOUIAD, F. HAMON, P. VILLECHAISE and X. MILHET - Philosophical Magazine Letters, 2010. 90(8): p. 611-620.
[21] R. GIRAUD, R., Z. HERVIER, J. CORMIER, G. SAINT-MARTIN, F. HAMON, X. MILHET and J. MENDEZ - Metallurgical and Materials Transactions A, 2013. 44A: p. 131-146.
[22] A. DLOUHY, M. PROBST-HEIN and G. EGGELER - Material Science and Engineering, 2001. A309-310: p. 278-282.
[23] M. PROBST-HEIN, A. DLOUHY and G. EGGELER - Acta Mater, 1999. 47(8): p. 2497-2510.
[24] M. BENYOUCEF, N. CLEMENT and A. COUJOU - Material Science and Engineering, 1993. A164: p. 401-406.

[25] B. FEDELICH, A. EPISHIN, T. LINK, H. KLINGELHÖFFER, G. KÜNECKE and P.D. PORTELLA - Superalloys 2012. 2012. Seven Springs, PA, USA: TMS.
[26] B. FEDELICH, B., A. EPISHIN, T. LINK, H. KLINGELHÖFFER, G. KÜNECKE, and P.D. PORTELLA - Computational Materials Science, 2012. 64: p. 2-6.
[27] R.C. REED, D.C. COX and C.M.F. RAE - Materials Science and Engineering, 2007. A 448: p. 88-96.
[28] J.K. TIEN and S.M. COPLEY - Met. Trans., 1971. 2: p. 215-219.
[29] J.-B. LE GRAVEREND, L. DIRAND, A. JACQUES, J. CORMIER, O. FERRY, T. SCHENK, F. GALLERNEAU, S. KRUCH and J. MENDEZ - Metallurgical and Materials Transactions A, 2012. 43A: p. 3946-3951.
[30] J.-B. LE GRAVEREND, A. JACQUES, J. CORMIER, O. FERRY, T. SCHENK and J. MENDEZ - Acta Materialia, 2015. 84: p. 65-79.
[31] H. HUFF and H. PILLHOFER - Superalloys 1988. 1988: TMS, Warrendale, PA.
[32] S. WANG, D.S. XU, N. MA, N. ZHOU, E.J. PAYTON, R. YANG, M.J. MILLS and Y. WANG - Acta mater, 2009. 57: p. 316-325.
[33] J. CORMIER - Phd Thesis, 2006, University of Poitiers - ISAE-ENSMA, Poitiers, France.
[34] W. CHEN and J.-P. IMMARIGEON - Scripta Materiala, 1998. 39(2): p. 167-174.
[35] B. FEDELICH, G. KUNECKE, A. EPISHIN, T. LINK and P. PORTELLA - Materials Science and Engineering, 2009. A 510-511: p. 273-277.
[36] L.M. KACHANOV - Isv. Akad. Nauk. SSR. Otd. Tekh. Nauk., 1958. 8: p. 26-31.
[37] N. MATAN, D.C. COX, P. CARTER, P.A. RIST, C.M.F. RAE and R.C. REED - Acta mater, 1999. 47(5): p. 1549-1563.
[38] M. MCLEAN and B.F. DYSON - Journal of engineering Materials and Technology, 2000. 122: p. 273-278.
[39] N.X. HOU, Z.X. WEN and Z.F. YUE - Materials Science and Engineering, 2009. A 510-511: p. 42-45.
[40] J. KOMENDA and P.J. HENDERSON - Scripta Materiala, 1997. 37(11): p. 1821-1826.
[41] J.-R. VAUNOIS, J. CORMIER, P. VILLECHAISE, A. DEVAUX and B. FLAGEOLET - 7th International Symposium on Superalloy 718 and Derivatives. 2010. Pittsburgh, PA, USA: TMS.
[42] R. GIRAUD, J. CORMIER, Z. HERVIER, D. BERTHEAU, K. HARRIS, J. WAHL, X. MILHET, J. MENDEZ and A. ORGANISTA - Superalloys 2012. 2012. Seven Springs, PA, USA.
[43] A. JACQUES and P. BASTIE - Phil. Mag., 2003. 83(26): p. 3005-3027.
[44] T. SCHENK, T., A. JACQUES, J.-B. LE GRAVEREND and J. CORMIER - in TMS 2015 Annual Meeting. 2015. Orlando, Fl, USA.
[45] J. BESSON, R. LE RICHE, R. FOERCH and G. CAILLETAUD - Revue Européenne des Eléments Finis, 1998. 7: p. 567-588.
[46] J.-B. LE GRAVEREND - PhD. Thesis 2013, ISAE-ENSMA & ONERA, Chatillon, France.
[47] A. MATTIELLO - PhD. Thesis, 2017, ISAE-ENSMA & ENS Cachan, Cachan, France.
[48] D. DYE, A. MA and R.C. REED - Superalloys. 2008. Seven Springs, Champion, PA, USA: TMS.
[49] C.M.F. RAE and R.C. REED - Acta mater, 2007. 55: p. 1067-1081.

AUTHORS

Jonathan Cormier received his Engineering diploma and his Doctoral degree in Mechanics of Materials both from ISAE-ENSMA in 2003 and 2006 respectively. Since 2002, he has been involved in various experimental and numerical studies on the deformation and damage processes of high temperature materials, with a special focus on the role of microstructure evolutions on the mechanical resistance of cast (SX/DS) and wrought superalloys and on the durability of TBC coatings under close-to-reality loading conditions (using unique burner rig experiments). Since 2007, he works as an Associate professor at ISAE-ENSMA in 2007 (Institut Pprime, UPR CNRS 3346, Futuroscope-Chasseneuil). He authored/co-authored over 50 international publications in these fields and he acts as a member of the Metallurgical and Materials Transactions A Board of review.

Florent Mauget received his engineering diploma in 2007 from Polytech'Orléans. He has worked at Institut Pprime since 2007 as an engineer. He designed and developped a new burner rig facility called MAATRE used to perform thermomechanical fatigue tests under hot gas flow. He is involved in studies on Ni-based superalloys behavior in close to realistic conditions as well as studies on the dammage mechanisms of thermal barrier coatings systems.

Jean-Briac le Graverend received his Engineering diploma from ISAE-ENSMA in 2009 and his PhD in Mechanics of Materials from ISAE-ENSMA and ONERA in 2013 during which he studied the anisothermal deformation and damage of Ni-based single crystal superalloys under conditions representative of in-service operation. After his graduation, he did a post-doc at Caltech during which he worked on characterizing the viscoelastic properties of electromechanical composites under temperature and electric field control. Since 2014, he works as an Assistant Professor within the department of Aerospace Engineering at Texas A&M University. His research goals are to predict the mechanical behavior of materials (metallic and ceramic) at high temperature by means of a multi-scale approach using experimental (high temperature mechanical testing, microstructure observation, tomography, and synchrotron radiation), theoretical (crystal plasticity, phase field, and incremental variational principle), and computational (FE simulation) tools.

Clara Moriconi received her Engineering diploma from ISAE-ENSMA in 2009 and her PhD in Mechanics of Materials from ISAE-ENSMA in 2012 during which she worked on modelling of fatigue crack propagation in gaseous hydrogen using cohesive zone elements and a specifically-designed material law. Since 2013, she has been working as a numerical methods engineer at TURBOMECA - a French manufacturer of gas turbine turboshaft engines for helicopters, in the field of creep and fatigue life prediction of turbine components. Her mission is to constantly strive to improve methods used for life prediction of TURBOMECA structures.

José Mendez, Doctor of Sciences from ENSMA and Director of Research at CNRS. He is involved in experimental studies on the fatigue damage mechanisms of metallic materials. His current fields of interest are: 1) Damage mechanisms of structural materials under monotonic and cyclic loading; 2) Relation between microstructure and mechanical properties (fatigue, creep-fatigue); 3) Aging effects; 4) Effect of temperature and environment (air, high vacuum) on fatigue properties; 5) Improvement of fatigue resistance by thin coatings or other surface treatments; 6) Microstructure optimisation of advanced materials: titanium alloys, nickel base superalloys, stainless steels, high strength steels. He authored or co-authored more than 120 publications in these fields.